ECOLOGY LETTERS

Ecology Letters, (2011) doi: 10.1111/j.1461-0248.2011.01712.x

LETTER

Scaling and structure of dicotyledonous leaf venation networks

Charles A. Price,[1*] Scott Wing[2] and Joshua S. Weitz[3,4*]

Abstract

There have been numerous attempts to derive general models for the structure and function of resource delivery networks in biology. Such theories typically predict the quantitative structure of vascular networks across scales. For example, fractal branching models of plant structure predict that the network dimensions within plant stems or leaves should be scale-free. However, very few empirical examples of such networks are available with which to evaluate such hypotheses. Here, we apply recently developed leaf network extraction software to a global leaf dataset. We find that leaf networks are neither entirely scale-free nor governed entirely by a characteristic scale. Indeed, we find many network properties, such as vein length distributions, which are governed by characteristic scales, and other network properties, notably vein diameter distributions, which are typified by power-law behaviour. Our findings suggest that theories of network structure will remain incomplete until they address the multiple constraints on network architecture.

Keywords

Allometry, biological networks, branching, characteristic scale, fractal, functional trait, scale free, scaling, venation network, xylem.

Ecology Letters, (2011)

INTRODUCTION

Identifying a general model built on physical first principles for the structure and function of fluid distribution networks has been a long-standing goal in biology. Most previous models have hypothesised that natural selection has optimised network geometry to perform some function, such as minimising resistance to hydraulic flow (Murray 1926; West *et al.* 1999), minimising structural material or blood volume (Murray 1926; Banavar *et al.* 1999), or maintaining biomechanical similarity across branching generations (McMahon & Kronauer 1976). Within a given optimisation framework, network theories typically predict the quantitative structure of networks across scales, e.g., across branching generations in a tree or leaf. All of the aforementioned models predict scale-free behaviour in some feature of the hierarchical branching network. For example, fractal branching models predict power-law scaling of xylem lengths (West *et al.* 1999), and radii (Murray 1926; West *et al.* 1999) within plant stems, with similar predictions by model extensions applied to the venation structure within leaves (Price & Enquist 2007; Price *et al.* 2007).

To date, empirical tests of these network theories in biology have largely focused on evaluating model predictions rather than on evaluating the purported mechanism by directly examining network structure (see discussion in Price *et al.* 2010a). For example, there has been an extended debate as to the form of the relationship between organism metabolic rate and mass. The debate centres around whether the scaling exponent is 2/3, 3/4 or even whether a power-law exists (Dodds *et al.* 2001; Savage *et al.* 2004; Kolokotrones *et al.* 2010), given the predictions of a 3/4 exponent resulting from West *et al.*'s fractal branching network model (West *et al.* 1997, 1999). Testing secondary rather than primary predictions of network geometry has largely been a matter of necessity: there exist few complete quantitative descriptions of physical network structure with which to test predictions. In mammals, there are a few dozen descriptions of cardiovascular networks from which the statistics of hierarchical side-branching can be estimated (Zamir 2001). No analogous studies of complete plant branching networks exist from which to estimate the statistical structure of xylem branching (Horn 2000). Within trees, the properties of xylem conduits have been studied extensively, providing partial views of xylem dimensions including cross-sections (Anfodillo *et al.* 2006; Savage *et al.* 2010; Weitz *et al.* 2006; Petit & Anfodillo 2009) and lengths (Tyree & Zimmerman 2002), but no whole-network measurements are available.

The status of the study of vein networks within leaves is similar, in that only a handful of attempts have been made to quantify the geometry of leaf networks (Canny 1990; McCulloh *et al.* 2003). Most instances of network analysis represent measurements of portions of the network, e.g. local vein density (Sack & Frole 2006; Brodribb *et al.* 2007; Blonder *et al.* 2010; Scoffoni *et al.* 2011), the side lobe of a leaf (Turcotte *et al.* 1998), the primary and sometimes secondary venation (Niinemets *et al.* 2007a,b), and the scaling of conduit diameter with vessel bundle diameter in the first few vein orders (Coomes *et al.* 2008). There have been a few attempts to quantify the geometry of entire networks, utilising automated image analysis algorithms on a handful of leaves (Bohn *et al.* 2002), or interactive approaches in small *Arabidopsis* leaves (Rolland-Lagan *et al.* 2009). Quantifying the geometry of entire leaf networks has remained elusive primarily because of the sheer number of measurements required and due the complexities of image analysis (Price *et al.* 2010b). This deficit in the availability of complete network information is unfortunate, given the central role leaves play in determining the hydrodynamic status, growth rate and fitness of plants (Lambers *et al.* 1998; Sack & Holbrook 2006).

[1]*School of Plant Biology, University of Western Australia, Crawley, Perth 6009, Australia*
[2]*Department of Paleobiology, National Museum of Natural History, Smithsonian Institution, Washington, D.C. 20013, PO Box 37012, USA*
[3]*School of Biology, Georgia Institute of Technology, Atlanta, GA 30332, USA*
[4]*School of Physics, Georgia Institute of Technology, Atlanta, GA 30332, USA*
**Correspondence: E-mail: charles.price@uwa.edu.au; jsweitz@gatech.edu*

To begin to address this void, we first developed a null model for the scaling properties of leaf vascular networks. The null model is based on numerous observations that angiosperm leaf networks typically have a reticulate structure (Sack *et al.* 2008; Blonder *et al.* 2010; Corson 2010; Katifori *et al.* 2010). Therefore, we assumed that leaf networks should have structural properties resembling lattices, in which each lattice cell can be thought of as analogous to an areole. However, we also anticipate that the patterning of veins may be irregular, and discuss how disorder may impact the distributions of vein dimensions we observe in specimens. We then compared the null model predictions to over 4 000 000 individual vein measurements obtained from the vein networks of 353 leaves representing 339 species in 72 angiosperm families (Tables S1–S4). To extract leaf network statistics, we applied image segmentation algorithms contained in the LEAF GUI software package to unmagnified leaf images (Price *et al.* 2010b), which allowed us to extract the position, width and length of each vein segment and its connectivity to other segments. We focused on three types of quantitative descriptions for our analysis due to their bearing on the aforementioned theories and our null models: (1) measures of local structure such as mean edge length (where 'edge' refers to the vein segment that occurs between branching points), mean intra-vein distance, and network density as a function of increasing leaf size; (2) aggregate measures for each leaf such as total network length or the total number of vein edges, as a function of increasing leaf size; and (3) the frequency distributions of edge lengths and diameters within each leaf.

As we demonstrate, leaf networks have a broad array of properties strongly consistent with our null model of a disordered lattice, including mean edge length, mean intra-vein distance, network density, and network length distributions. For example, we find that all of the local properties we consider are statistically invariant with respect to leaf size, and are strongly consistent with an observed structure driven by a characteristic scale, which is probably linked to diffusive length scales that may be species specific. We define the characteristic scale as the average length scale of the network as revealed in the geometry of its veins and/or areoles. Moreover, we find that all the aggregate properties increase as a linear function of leaf size, i.e., as the leaf gets bigger, there are more network edges, but their properties remain statistically invariant. However, the leaf networks we examine do have properties that are consistent with a scale-free design. In particular, we find that overall, the distributions of vein widths are better fit by power-laws than by exponentials, suggesting that the need for veins to deliver water and nutrients across a hierarchical network leads to a (partially) self-similar structure. Taken as a whole, our empirical analysis suggests that the constraints of mass flow require vein radii to connect hierarchically in a way that is scale-free ('fractal-like'). However, we also find that the majority of structural features, including the length scale of the veins that underlie the geometry of the venation network, do not change systematically across species with different leaf sizes. We conclude by discussing the functional significance of our empirical findings of scale-free designs and characteristic scales within leaf networks and suggest the need to revisit optimisation theories of resource delivery networks in biology.

MATERIAL AND METHODS

Image metadata and analysis

Our dataset contains observations for leaves representing 353 individual cleared leaves of which there are 339 distinct species, with 29 Magnoliids, and 310 Eudicots (Table S1). These data come from the National Cleared Leaf Collection housed at the Museum of Natural History, Smithsonian Institution. The leaves we selected come from a collection of over 13 000 individual specimens. The medium in which these leaves were originally mounted is unfortunately deteriorating, damaging many of the leaves. As a consequence, most of the images are unsuitable for *whole* leaf network analysis. The analysis of approximately one specimen per species reflects the availability of suitable images in the collection.

We went through the entire collection, selecting only the best images for our analyses. Images were selected based on three criteria: (1) their leaves were intact (free from tears or other damage) or nearly so; (2) image resolution was sufficient to resolve most of the higher order veins, and; (3) the contrast between leaf veins, areoles and background was significant enough for our network extraction algorithms to resolve their structure. To analyse the images, we wrote a series of image analysis algorithms to extract network statistics from leaf scans using the Matlab software programme. These algorithms have been compiled into a graphical user interface for public use, with an accompanying manuscript (Price *et al.* 2010b), user manual and demonstration videos (http://www.leafgui.org). The result of applying these algorithms to an individual leaf image is a set of connected edges, along with additional information on their dimensions, position and connectivity (see Fig. 1a–d for an illustration of these steps for a specimen of *Gaultheria oppositifolia* Hook. f.).

The resulting leaf network is represented as a set of connected edges, of which each edge has an assumed cylindrical shape. This is a common assumption in plant vascular analyses underlying almost all theoretical and empirical treatments; for example, measurements of sap flow rates often assume that flow can be approximated by the Hagen–Poiseuille equation, which assumes a cylindrical conduit (Tyree & Ewers 1991). Each cylindrical edge can then be described by two linear dimensions, length and diameter, which then enable the calculation of surface area and volume of the cylinder.

To calculate the dimensions of each individual cylindrical edge, we first apply a series of thresholding and cleaning steps (see Price *et al.* 2010b for a detailed description) to a cleared leaf image (Fig. 1a). We convert the original RGB image to grayscale (0–255), then utilise both global and local adaptive thresholding approaches to yield a binary representation of the leaf vein network where veins are represented by 1's and non-vein areas are represented by 0's (Fig. 1b). Global thresholding sets all image pixels greater than a user set value to foreground (1's), and all others to background (0's). Adaptive thresholding is similar in principle, but takes into account the uneven illumination of many leaf images. To correct for this, adaptive thresholding uses a local square window, the size of which is set by the user (in pixels). This window is then automatically moved across the image and pixels are separated into foreground and background according to whether their values, I, are greater than the value $I_m - X$, where I_m is the mean intensity value in the local window and X is a threshold offset level preset by the user (usually set close to 0). Subsequent application of a distance transformation results in a representation of the network where the distance from each vein pixel, to the nearest non-vein pixel is recorded (Fig. 1c). We then skeletonise the entire image, resulting in a single pixel wide representation of the network (Fig. 1d). Nodes (red pixels, Fig. 1d) and tips (yellow pixels, Fig. 1d) are identified automatically. Edge skeletons are then identified as those pixels between nodes or between a node and a tip (light blue pixels, Fig. 1d). Within an individual edge, the value of the distance

transformation within each skeleton pixel corresponds to an estimate of the radius at that pixel. We take the mean of all the pixel radii within a given edge and multiply this value by two to arrive at an estimate for the edge diameter. Each edge length is calculated by walking along the edge counting one unit for pixels that share a border, and $\sqrt{2}$ for pixels that touch on their corners.

Null model: leaf network as a honeycomb lattice with disorder

The functional basis for our set of null models is the observation that, relative to bulk flow through conduits, there exists a large resistance to flow of solution from xylem termini to sites of evaporation (Brodribb *et al.* 2007; Noblin *et al.* 2008), or from the sites of photosynthesis to phloem conduits (Raven 1994), which restricts the distance over which such flow can occur. If Γ is the length scale at which breakdown of flow occurs due to diffusion and/or other limitations, areoles should have a characteristic scale $l_C < \Gamma$. We model areoles as forming regular structures, and hence a leaf as a series of veins that make up the edges in a lattice, such that l_C is the length of an average edge and, in the case of a honeycomb lattice, also the distance from a node to the centre of the areole (see Fig. 2 and Appendix S1 in Supporting Information). The choice of a honeycomb structure is based on visual inspection suggesting that regular polygons similar in shape to hexagons well describe the shape of areoles in many of the leaves we considered, and areoles of this shape are common in non-monocot angiosperms (Ellis *et al.* 2009). However, we also consider other lattice models in which the basis lattice unit is a square and a triangle (see Appendix S1).

In general, the use of a lattice model simplifies predictions of how local and aggregate network features change with system size, because the scale l_C can be used to make first order predictions. Here, we explain the general scaling relationships amongst network features using dimensional analysis, and note that the particular prefactors in the scaling relationships vary between lattice types, e.g., honeycomb, square or triangular lattices (see Table S5, Appendix S1). First, the number of edges per unit area, or edge density, ρ_0, should be proportional to l_C^{-2}, i.e., $\rho_0 \sim l_C^{-2}$. Next, the network length density, ρ_1, is defined as the average length of edges multiplied by the edge density, or $\rho_1 = l_C \rho_0 \sim l_C^{-1}$. Likewise, as is apparent in Fig. 2, the mean distance of points within a lattice element to the nearest edge is proportional to the edge length, i.e., $d \sim l_C$. Finally, the number of edges, N_E, and nodes, N_N, increases linearly with the number of lattice elements. Hence, the scaling of these aggregate network measures can be found as the product of the leaf area and edge density, $N_E \sim N_N \sim A_L\, l_C^{-2}$. Similarly, the total network length, L_{tot}, is the product of the number of edges and average edge length, or $L_{tot} \sim A_L\, l_C^{-1}$.

Note that visual investigation of areoles within individual specimens suggests that any regular lattice shape only partially captures the complexity of areoles. In a purely lattice-based model, edge lengths would be identical, or at least unimodal and narrowly distributed around the characteristic scale, l_C. Here, we present an alternative hypothesis. We propose that veins may be generated by a process that includes a random component, such that growing veins stop and/or branch at random with a constant probability per unit length, p. Given random branching and/or stopping, veins lengths will follow an exponential distribution, such that $P(l) = pe^{-pl}$. We identify this average length, $l_C = 1/p$ with the characteristic scale explained above. Hence, an alternative hypothesis is that empirical edge length distributions should be exponential with characteristic scale l_C. Note that the length of

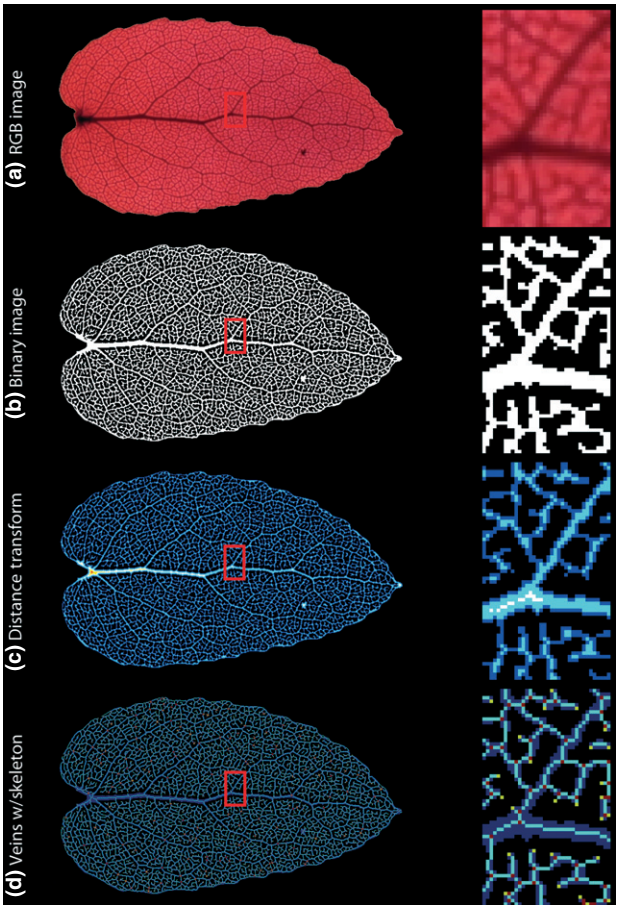

Figure 1 Sequence of images representing several stages of the LEAF GUI image segmentation, vein extraction, and measurement algorithms: Panel (a) represents a raw image from a *G. oppositifolia* leaf. Panel (b) displays the results from a combination of local and global thresholding approaches, Panel (c) represents the results of distance transform algorithms on the binary image in (b). Panel (d) is the vein network (dark blue) with the image skeleton (light blue) with nodes (red) and tips (yellow) identified.

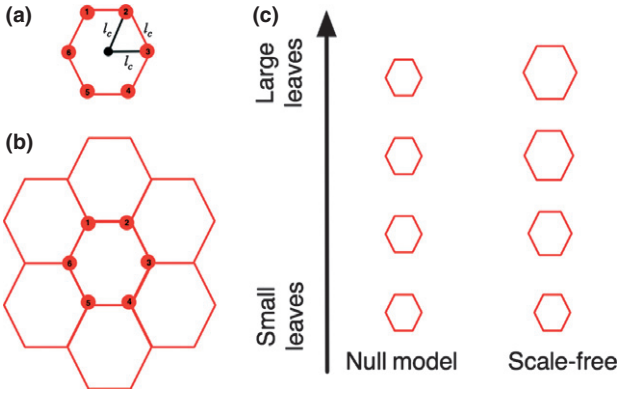

Figure 2 Illustration of the characteristic scale of a lattice. Panel (a) represents the characteristic scale of a lattice, using a honeycomb lattice element for which the edge distance is equal to that of the distance from any node to the centre. Panel (b) depicts how individual lattice elements combine to create an entire lattice. Panel (c) depicts how lattice elements may not necessarily increase in size (null model) or increase in size (in a scale-free model) as the leaf size increases.

network segments within river networks are exponentially distributed, presumably due to random coalescence processes (Dodds & Rothman 1999), in support of our current approach.

Statistical analysis: bivariate relationships

Bivariate relationships among the majority of the aforementioned traits were analysed by fitting ordinary least squares (OLS) or standardised major axis (SMA) regression lines to linear or log scaled variables. Often in allometric analyses, SMA is preferred (Warton *et al.* 2006), particularly when the measurement error in both the ordinate and abscissa is proportional, and a few of the relationships we explored warrant the use of SMA. However, the image segmentation algorithms we utilise are likely subject to significantly more error than whole leaf area measures, thus when the independent variable is leaf area, we use OLS; alternatively, we use SMA. For most of the relationships we report, the difference between OLS and SMA slopes would be minor anyway, considering the high correlation coefficients we observe (SMA slope = OLS slope/$\sqrt{}$(OLS R^2).

Statistical analysis: maximum likelihood estimation of distribution parameters

Vein dimension distributions were fit to exponential and power-law distributions. The maximum likelihood estimate (MLE) for the rate parameter (γ) for the exponential distribution is simply $1/\langle x\rangle$, and the log likelihood ($\log L$) is given by, $\log L = N(\log\langle \gamma\rangle - 1)$, where N is the sample size. The MLE for the power-law model is given by, $\log L = N\log\left(\frac{\gamma-1}{x_{MIN}^{1-\gamma}}\right) - \gamma\sum_{i=1}^{N}\log x_i$, where X_{MIN} is the minimum value of X, γ is the scaling exponent, and $\left(\frac{\gamma-1}{x_{MIN}^{1-\gamma}}\right)$ is the normalising constant. We follow the recent work of Clauset *et al.* (2009) in using MLE's for power-law fits. To compare the two models, we used the method of maximum likelihood to estimate the model parameters and likelihood. We then used Akaike's information criterion (AIC) to evaluate which model provided a better fit to the data: AIC = $2k - 2\log L$ where k is the number of model parameters and L is the likelihood. For the exponential model, $k = 1$, whereas for the power-law, $k = 2$.

RESULTS

Network properties of 353 leaf venation networks

Our dataset exhibits multiple orders of magnitude variation in aggregate network size (Table S2). For example, the total network length ranges from ~200 mm to ~18500 mm, spanning nearly 2 orders of magnitude (see Fig. S1a). However, despite this variation, we observe far less variation in local network structure. For example, the average edge length ranges from ~0.11 mm to ~0.52 mm and shows a clear central tendency (Fig. S1b). Hence, we have preliminary evidence that local network properties are de-coupled from total size. Next, we evaluate the extent to which the lattice model is an appropriate descriptor of our vein dimension data.

Scaling of local measures of network structure

Recall that our null model is that of a lattice with characteristic scale l_C (see Fig. 2). Hence, we can evaluate the hypothesis of the existence of a characteristic scale in leaves by determining if l_C, edge density ρ_0, and the average distance from non-vein tissue to the network d, are all uncorrelated with leaf area, A_L (see Fig. 2c). In contrast, if the basis unit of the lattice changed in size as leaf area increased, then we would expect to see correlations between these local measures of lattice structure and leaf area (see Fig. 2c). We find that, l_C, d and ρ_1 are all invariant with A_L or nearly so (Table 1, Fig. 3), in accord with a scale-invariant lattice. Moreover, we observe a positive scaling between l_C and d as expected for a lattice (Table 1). The leaf level mean value of d/l_C varied from 0.158 to 0.39 with a mean value of 0.295 (standard deviation = 0.037), whereas the expected mean value for d/l_c for a honeycomb lattice is ~0.29; for a square lattice is ~0.17, and for a triangular lattice is ~0.10 (Appendix S1). Hence, a lattice, and in particular, a honeycomb lattice is a useful null model for baseline predictions, in that the distance from areoles to veins is largely determined by the characteristic length scale of a leaf. Note that our values for network density (Fig. 3, Panel E) overlap with, but are generally lower than those reported for leaves imaged under 20× (Boyce *et al.* 2009) or 40× (Sack & Frole 2006) magnification. We suspect that these differences are due to the fact that our images are unmagnified photographs, which may not resolve all of the very smallest veins, yet which include all major veins.

Scaling of aggregate measures of network structure

The next set of predictions from our null model is that as leaves increase in size, their characteristic length scale does not change, but the number of lattice elements (analogous to areoles) along with associated edges and nodes increases in proportion to leaf area (see Fig. 2b). Across all leaves, we find that the scaling relationships between number of edges N_E, the number of nodes N_N and the total network length L_{TOT} with respect to variation in A_L are all well

Table 1 Regression statistics for interspecific scaling relationships: The *P*-value indicates the probability the observed slope is not different from the null slope resulting from the isometric lattice model. Note, as indicated in the Methods, OLS regression was used in those cases when error in the independent variable (leaf area) was thought to be substantially less than that in the dependent variable

Dependent variable	Independent variable	R^2	Slope	Low CI	Upp CI	Interc	Null slope	*P*	Method	Figure
Log number of edges (N_E)	Log leaf area (A_L)	0.83	0.97	0.92	1.01	0.68	1	0.15	OLS	4a
Log number of nodes (N_N)	Log leaf area (A_L)	0.81	0.97	0.92	1.02	0.48	1	0.19	OLS	4b
Log total network length (L_{TOT})	Log leaf area (A_L)	0.93	0.96	0.94	0.99	0.25	1	0.01	OLS	4c
Log number of edges (N_E)	Log number of nodes (N_N)	0.99	0.99	0.98	0.99	0.25	1	0	SMA	4d
Mean edge length (l_C)	Log leaf area (A_L)	0.002	−0.01	−0.04	0.02	−0.53	0	0.43	OLS	3a
Mean distance to edge (d)	Log leaf area (A_L)	0.03	0.03	0.01	0.06	−1.22	0	0.003	OLS	3b
Network density (ρ_1)	Log leaf area (A_L)	0.02	−0.04	−0.06	−0.01	0.25	0	0.01	OLS	3c

OLS, ordinary least squares.

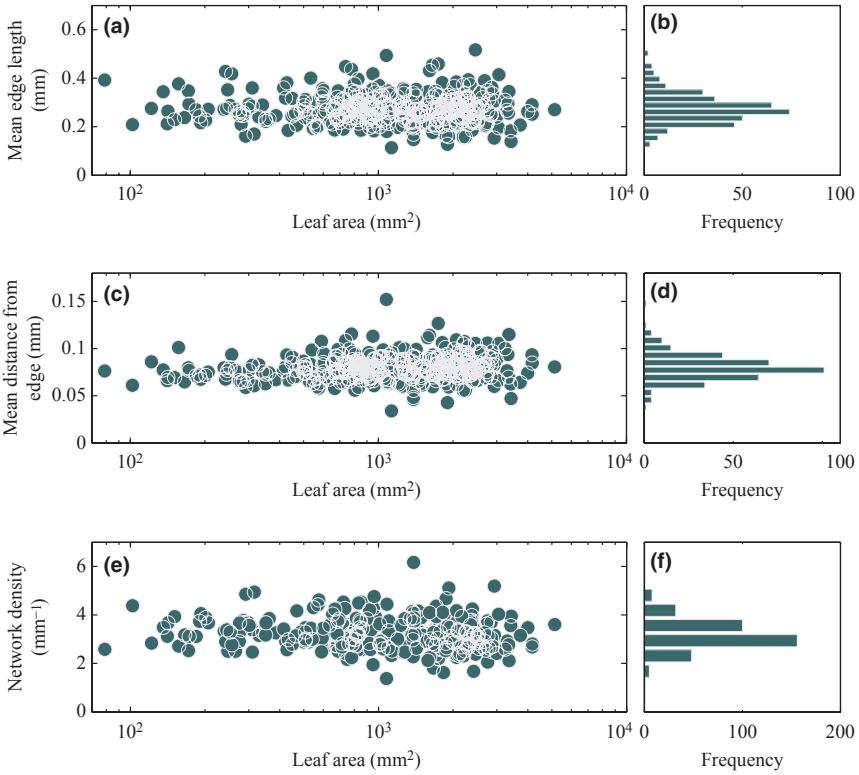

Figure 3 Bivariate plots of mean edge length (l_C, Panel a), mean distance from edge (d, Panel c) and network density (ρ_1, Panel e) all as a function of leaf area (A_L) (statistics given in Table 1). Each point corresponds to an individual leaf. Note that while variability exists in the dependent variables, that variability is not explained by changes in leaf area. Panels (b), (d) and (f) are histograms of the data presented in Panels (a), (c) and (e) respectively. Note that the distributions are modal, consistent with the definition for type B invariance as defined by Charnov (Savage *et al.* 2006).

approximated by power-laws with exponents all very close to one (Fig. 4, Table 1). The scaling of N_N with N_E is close to unity (Fig. 5) as is expected for planar networks, and the ratio of total number of edges to nodes was highly conserved across leaves, with a mean value of 1.58 and a variance of 0.003. The scaling of N_E and N_N with A_L are statistically identical (Table 1) and only marginally different from one. In addition, the scaling of both L_{TOT} and D_{TOT} are nearly isometric with A_L (Table 1). Hence, the evidence suggests that the total size of the venation network grows linearly with leaf size, at least across the range of leaf size we have examined.

Distribution of lengths and diameters are consistent with both a characteristic scale null model and scale-free connectivity

The lattice null model is consistent with the scaling of both local network structure and total network size as a function of leaf area. However, visual inspection of leaves (as in Fig. 1) makes it apparent that there is disorder in venation networks. Here, we quantify disorder by analysing the probability distributions of vein dimensions within leaves. A preliminary look at the probability distribution functions of both vein lengths and vein diameters for a few leaves indicated that both were decreasing functions of size, and linear on log-linear and log-log scales respectively (see Supplementary File S1, which includes visual depictions of distributions for vein lengths and diameters for all 353 specimens). Any number of candidate models might be suggested; however, both the exponential and power-law models have been invoked to explain the scaling of resource delivery networks, thus for each leaf we compared the fit of both models for the distributions of vein lengths and diameters. The distribution of vein lengths was better fit by an exponential model rather than by a power-law model 100% of the time (353/353 cases). In contrast, the distribution of vein diameters was better fit by a power-law distribution in 273/353 cases or 77% of the time. (Fig. 5, Supplementary File S1, Table S3). Thus, leaves typically possess a mixture of frequency distributions underlying their network geometry that typify characteristic scale models (exponential fits) and scale-free models (power-laws) (see Methods for fitting procedures).

Statistical analysis: comparing prefactor predictions of scaling relationships to those obtained from lattice models

The prior scaling results hold for lattice models in which the size of the lattice element does not increase with leaf area. We found that the average distance to the closest vein agrees with that of a honeycomb lattice model prediction. Here, we further evaluate the utility of the honeycomb lattice by its ability to predict the pre-factors of the remainder of the scaling relationships, and compare it with lattice model alternatives in which areoles have a characteristic four-sided (square) or three-sided (triangle) shape. In each case, we first estimate the characteristic length scale by finding the mean edge length in a leaf. Then, we utilise this length scale to predict the following network features: number of edges per area (ρ_0); length of edges per area (ρ_1), mean distance to nearest edge (d), total number of edges (N_E), total number of nodes (N_N), and total network length (L_{TOT})

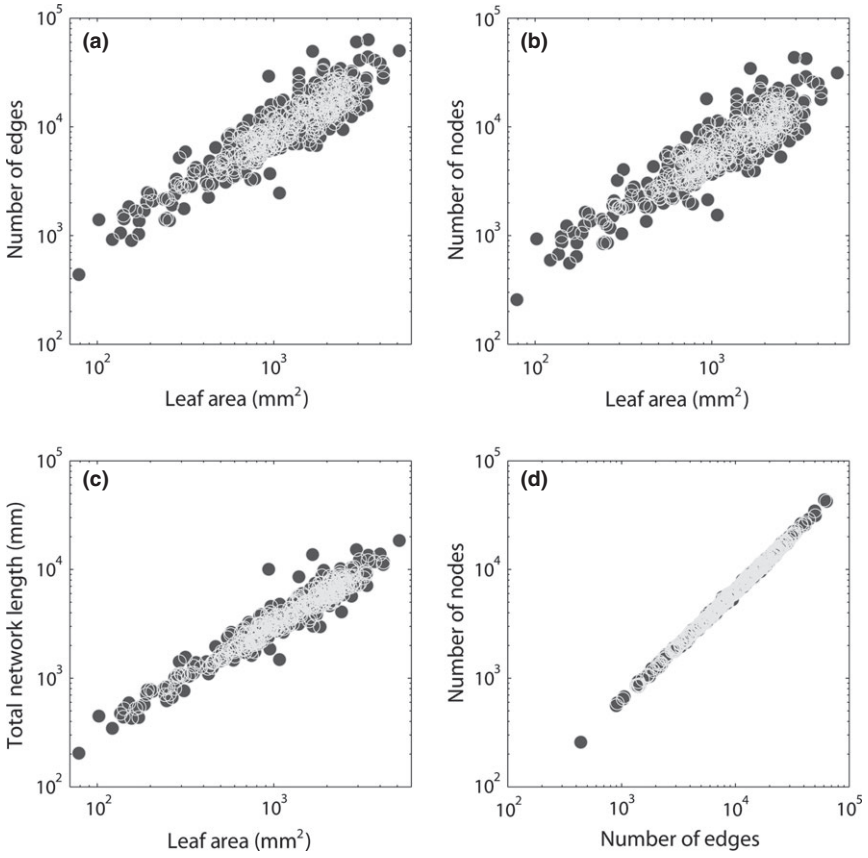

Figure 4 Number of edges (N_E), number of nodes (N_N) and total network length (L_{TOT}) as a function of leaf area (A_L) (Panels a–c), N_N vs. N_E (Panel d). Each point corresponds to a single leaf. Note regression slopes for all four relationships are statistically indistinguishable from one (or nearly so), consistent with the null isometric lattice model (Table 1).

(see Appendix S1 for derivations of these relationships). We compare predicted values for each quantity with the measured value (see Appendix S1). The honeycomb lattice model had the lowest sum of squared deviations from the 1:1 line in all six comparisons further demonstrating its usefulness as a null model for dicot leaf network structure (Figs. S2–S7, Appendix S1). However, we note that systematic deviations were observed in the prediction for the number of edges per unit area for all models (which lead to corresponding deviations for the total number of edges and the total length of edges). Such deviations are expected given that the networks we measure are hierarchical and have many freely ending veinlets. Incorporating such features into a null model is an important target for future work.

DISCUSSION

Understanding biological processes within a particular system is highly dependent on the scale of inquiry (Levin 1992). Within physical networks, characteristic scales have previously been found to govern material properties such as hydrodynamic flows in planar river networks (Rodriguez-Iturbe & Rinaldo 1997; Dodds & Rothman 1999); however, it has remained an open question as to whether such findings would apply to planar networks of biological origin. Here, we have shown that many components of leaf networks, including vein lengths and intra-vein distances, are also well-described by a characteristic length scale. Moreover, many aspects of leaf networks are consistent with a null model of a simple isometric honeycomb lattice: all of the scaling relationships we measured (Table 1) are in agreement (or nearly so) with the null model predictions, save the frequency distribution of edge diameters. In addition, the expected values for the lattice prefactors for a honeycomb lattice were superior to the other 2D lattice types we considered (Appendix S1). In contrast, recent work (Scoffoni *et al.* 2011) with a small group of 10 species has shown that major veins, identified utilising classical vein ranking approaches (Ellis *et al.* 2009), show decreasing density with increasing leaf area, while minor veins show no trend, consistent with our findings. Thus, the spacing of major and minor vein components may be somewhat decoupled.

Biologically, the finding of characteristic scales suggests that as leaves increase in size, much of their geometry remains fixed, and is probably driven by hydrodynamic constraints between photosynthetic tissue and the vein network (Zwieniecki *et al.* 2002; Boyce *et al.* 2009). We hypothesise that this length scale is determined by solution transport limitations between veins and sites of evaporation (Brodribb *et al.* 2007; Noblin *et al.* 2008) or from the sites of photosynthesis to phloem conduits (Raven 1994), and may differ between species, but is invariant with changes in leaf size across species. This is analogous to the finding that channels within river networks tend to be spaced by a characteristic length scale deriving from the assumption of uniform drainage density, i.e., rainfall falls everywhere and must flow out of the system (Rodriguez-Iturbe & Rinaldo 1997). In the case of leaves, assuming a homogeneous distribution of chloroplasts or of stomates

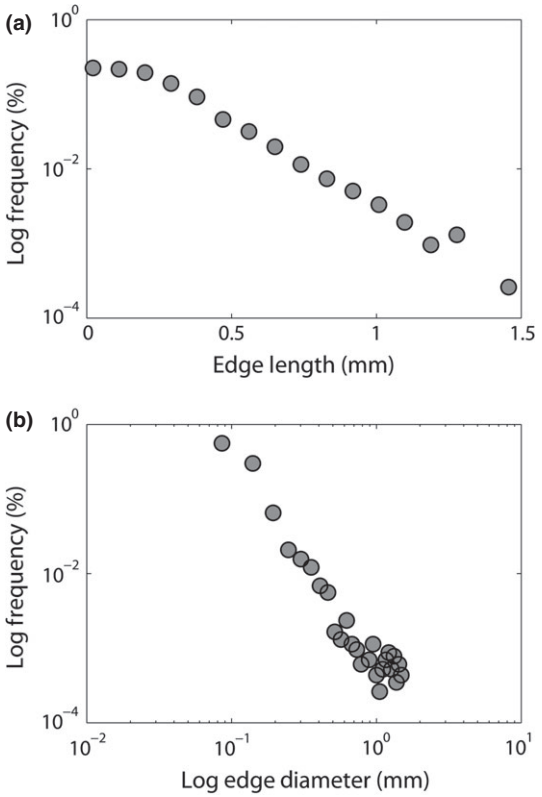

Figure 5 Frequency distributions of the edge lengths (Panel a) and edge diameters (Panel b) for a *Vismia brasiliensis* (Choisy) leaf from the image collection. The data in Panel (a) are linear on a log-linear scale, consistent with an exponential distribution, while the data in Panel (b) are linear on log-log axes, consistent with power-law behaviour (see Materials and Methods for fitting procedures). While we have displayed the distributions for a single leaf for clarity here, a file with all 353 distributions is available in the online SI (Supplementary File S1) and MLE statistics are available in Table S3.

suggests a mechanistic basis for a similar result. Moreover, a characteristic spacing of veins ensures that lamina are well supplied and able to cope with the water losses concurrent with CO_2 acquisition (Noblin *et al.* 2008).

A full accounting of the consequences of fluid transport in leaves must account for bulk flow in veins, diffusion outside vein system through the porous mesophyll, and diffusion of water vapour through stomatal pores. While there is no trend in mean vein size or intra-vein distance with leaf size in our dataset, there exists variation around the mean (Fig. 3). We suspect that this variation represents species level variability in vein porosity, the geometry and packing of mesophyll space, and stomatal dimensions. It will be of interest to learn, for example, if the residual variation in Fig. 3a–c is explained by systematic variation in mesophyll dimensions, stomatal size and/or number, or some other functional constraint.

Our finding that vein diameter distributions are better fit by power-laws supports the notion that hierarchical aspects of the network must change as leaves grow, without respect to a particular scale. Due to the constraints of mass conservation, hydrodynamic flow necessitates a network hierarchy to ensure that all potential sites of photosynthesis are supplied (Murray 1926; LaBarbera 1990). Thus, on the one hand, the network must develop in such a way that it is always close to the chloroplasts and/or stomates. On the other hand, the network veins must taper in a way that can sustain flow from relatively large petioles to much smaller veins surrounding areoles. The influence of these respective demands on the structure of the leaf networks is most clearly revealed in the differences in the frequency distributions of vein lengths and diameters (Fig. 5, Supplementary File S1). This is the first instance of which we are aware that a mixture of frequency distributions have been described underlying the scaling of biological networks. It will be of interest to see if this pattern is repeated in biological networks at other scales and subject to different physical constraints.

The finding of a statistically invariant and also biophysically relevant length-scale mixed with scale-free network properties stands in contrast to a suite of optimisation theories that predict a purely fractal branching structure of optimal resource delivery networks (West *et al.* 1997, 1999; Banavar *et al.* 1999; Price & Enquist 2007). Although several of these models (West *et al.* 1997, 1999) were not intended to be applied to leaves *per se*, our findings do stress the importance of empirical verification of purported fractal network geometry for other physical networks, such as whole plants or animals.

There are many factors that could explain the discrepancy between prior theory and data. Importantly, most previous optimisation theories of biological networks have assumed that networks have evolved to minimise a single quantity, such as total energy expended in maintaining the network, or alternatively, total network resistance. Real networks have evolved under multiple selection pressures. The structure of leaf venation networks impacts numerous traits related to leaf function such as, whole tree resistance (Sack & Holbrook 2006), photosynthetic rates (Brodribb *et al.* 2007), leaf longevity (Onoda *et al.* 2011) and the robust functioning of photosynthesis (Zwieniecki *et al.* 2002). With respect to the last of these examples, a number of recent papers have shown that loops within a vein network confer redundancy to xylem flow in the face of leaf damage (Sack *et al.* 2008; Corson 2010; Katifori *et al.* 2010). Hence, in the case of leaf venation networks, there are many classes of constraints that might reasonably be expected to be included in future theories of optimal branching. Although our results may stand in contrast to pure scaling predictions derived from a number of prior theories, we envision that the complexities in the current dataset will inspire theoretical and applied work while marking a new standard for testing optimal networks theories by direct comparison with biological network structure.

ACKNOWLEDGEMENTS

C.A.P. and J.S.W. acknowledge the support of the Defense Advanced Research Projects Agency under grant HR0011-05-1-0057. J.S.W. holds a Career Award at the Scientific Interface from the Burroughs Welcome Fund. S.L.W. acknowledges Dane Miller, Ian Tom, Erika Gonzalez, and Smithsonian volunteers who photographed specimens for this project and have helped with conservation of the cleared leaf collection. John Raven and Cathy Price provided helpful comments on an earlier version of this manuscript. The authors thank the three anonymous reviewers for their valuable comments and suggestions.

AUTHORSHIP

CAP and JSW designed the study, developed the theory and performed the analysis. SLW provided the leaf images, and contributed to theory development. All authors contributed to the writing and revising of the manuscript.

REFERENCES

Anfodillo, T., Carraro, V., Carrer, M., Fior, C. & Rossi, S. (2006). Convergent tapering of xylem conduits in different woody species. *New Phytol.*, 169, 279–290.

Banavar, J.R., Maritan, A. & Rinaldo, A. (1999). Size and form in efficient transport networks. *Nature*, 399, 130–132.

Blonder, B., Violle, C., Bentley, L.P. & Enquist, B.J. (2010). Venation networks and the origin of the leaf economics spectrum. *Ecol. Lett.*, 14, 91–100.

Bohn, S., Andreotti, B., Douady, S., Munzinger, J. & Couder, Y. (2002). Constitutive property of the local organization of leaf venation networks. *Phys. Rev. E*, 65, 12.

Boyce, C.K., Brodribb, T.J., Feild, T.S. & Zwieniecki, M.A. (2009). Angiosperm leaf vein evolution was physiologically and environmentally transformative. *Proc. R. Soc. B-Biol. Sci.*, 276, 1771–1776.

Brodribb, T.J., Feild, T.S. & Jordan, G.J. (2007). Leaf maximum photosynthetic rate and venation are linked by hydraulics. *Plant Physiol.*, 144, 1890–1898.

Canny, M.J. (1990). Tansley Review No. 22. What becomes of the transpiration stream? *New Phytol.*, 114, 341–468.

Clauset, A., Shalizi, C.R. & Newman, M.E.J. (2009). Power-law distributions in empirical data. *Siam Rev.*, 51, 661–703.

Coomes, D.A., Heathcote, S., Godfrey, E.R., Shepherd, J.J. & Sack, L. (2008). Scaling of xylem vessels and veins within the leaves of oak species. *Biol. Lett.*, 4, 302–306.

Corson, F. (2010). Fluctuations and redundancy in optimal transport networks. *Phys. Rev. Lett.*, 104, 4.

Dodds, P.S. & Rothman, D.H. (1999). Unified view of scaling laws for river networks. *Phys. Rev. E*, 59, 4865–4877.

Dodds, P.S., Rothman, D.H. & Weitz, J.S. (2001). Re-examination of the "3/4-law" of metabolism. *J. Theor. Biol.*, 209, 9–27.

Ellis, B., Daly, D.C., Hickey, L.J., Johnson, K.R., Mitchel, J.D., Wilf, P. *et al.* (2009). *Manual of Leaf Architecture*. Cornell University Press, Ithaca.

Horn, H.S. (2000). Twigs, trees, and the dynamics of carbon in the landscape. In: *Scaling in Biology* (eds Brown, J.H. & West, G.B.). Oxford University Press, Oxford, pp. 199–220.

Katifori, E., Szollosi, G.J. & Magnasco, M.O. (2010). Damage and fluctuations induce loops in optimal transport networks. *Phys. Rev. Lett.*, 104, 4.

Kolokotrones, T., Savage, V., Deeds, E.J. & Fontana, W. (2010). Curvature in metabolic scaling. *Nature*, 464, 753–756.

LaBarbera, M. (1990). Principles of design of fluid transport systems in biology. *Science*, 249, 992–1000.

Lambers, H., Chapin, F.S. & Pons, T.L. (1998). *Plant Physiological Ecology*. Springer, New York.

Levin, S.A. (1992). The problem of pattern and scale in ecology. *Ecology*, 73, 1943–1967.

McCulloh, K.A., Sperry, J.S. & Adler, F.R. (2003). Water transport in plants obeys Murray's law. *Nature*, 421, 939–942.

McMahon, T.A. & Kronauer, R.E. (1976). Tree structures: deducing the principle of mechanical design. *J. Theor. Biol.*, 59, 443–466.

Murray, C.D. (1926). The physiological principle of minimum work. I. The vascular system and the cost of blood volume. *Proc. Nat. Acad. Sci.*, 12, 207–214.

Niinemets, U., Portsmuth, A., Tena, D., Tobias, M., Matesanz, S. & Valladares, F. (2007a). Do we underestimate the importance of leaf size in plant economics? Disproportional scaling of support costs within the spectrum of leaf physiognomy. *Ann. Bot.*, 100, 283–303.

Niinemets, U., Portsmuth, A. & Tobias, M. (2007b). Leaf shape and venation pattern alter the support investments within leaf lamina in temperate species: a neglected source of leaf physiological differentiation? *Funct. Ecol.*, 21, 28–40.

Noblin, X., Mahadevan, L., Coomaraswamy, I.A., Weitz, D.A., Holbrook, N.M. & Zwieniecki, M.A. (2008). Optimal vein density in artificial and real leaves. *Proc. Natl. Acad. Sci. USA*, 105, 9140–9144.

Onoda, Y., Westoby, M., Adler, P.B., Choong, A.M.F., Clissold, F.J., Cornelissen, J.H.C. *et al.* (2011). Global patterns of leaf mechanical properties. *Ecol. Lett.*, 14, 301–312.

Petit, G. & Anfodillo, T. (2009). Plant physiology in theory and practice: an analysis of the WBE model for vascular plants. *J. Theor. Biol.*, 259, 1–4.

Price, C.A. & Enquist, B.J. (2007). Scaling mass and morphology in leaves: an extension of the WBE model. *Ecology*, 88, 1132–1141.

Price, C.A., Enquist, B.J. & Savage, V.M. (2007). A general model for allometric covariation in botanical form and function. *Proc. Nat. Acad. Sci.*, 104, 13204–13209.

Price, C.A., Gillooly, J.F., Allen, A.P., Weitz, J.S. & Niklas, K.J. (2010a). The metabolic theory of ecology: prospects and challenges for plant biology. *New Phytol.*, 188, 696–710.

Price, C.A., Symonova, O., Mileyko, Y., Hilley, T. & Weitz, J.S. (2010b). Leaf extraction and analysis framework graphical user interface: segmenting and analyzing the structure of leaf veins and areoles. *Plant Physiol.*, 155, 236–245.

Raven, J.A. (1994). The significance of the distance from photosynthesizing cells to vascular tissue in extant and early vascular plants. *Bot. J. Scotland*, 47, 65–81.

Rodriguez-Iturbe, I. & Rinaldo, A. (1997). *Fractal River Basins: Chance and Self-Organization*. Cambridge University Press, New York.

Rolland-Lagan, A.G., Amin, M. & Pakulska, M. (2009). Quantifying leaf venation patterns: two-dimensional maps. *Plant J.*, 57, 195–205.

Sack, L. & Frole, K. (2006). Leaf structural diversity is related to hydraulic capacity in tropical rain forest trees. *Ecology*, 87, 483–491.

Sack, L. & Holbrook, N.M. (2006). Leaf Hydraulics. *Ann. Rev. Plant Biol.*, 57, 361–381.

Sack, L., Dietrich, E.M., Streeter, C.M., Sanchez-Gomez, D. & Holbrook, N.M. (2008). Leaf palmate venation and vascular redundancy confer tolerance of hydraulic disruption. *Proc. Natl. Acad. Sci. USA*, 105, 1567–1572.

Savage, V.M., Gillooly, J.F., Woodruff, W.H., West, G.B., Allen, A.P., Enquist, B.J. *et al.* (2004). The predominance of quarter-power scaling in biology. *Funct. Ecol.*, 18, 257–282.

Savage, V.M., White, E.P., Moses, M.E., Ernest, S.K.M., Enquist, B.J. & Charnov, E.L. (2006). Comment on "The illusion of invariant quantities in life histories". *Science*, 312, 198.

Savage, V.M., Bentley, L.P., Enquist, B.J., Sperry, J.S., Smith, D.D., Reich, P.B. & von Allmen, E.I. (2010). Hydraulic trade-offs and space filling enable better predictions of vascular structure and function in plants. *Proc. Natl. Acad. Sci. U.S.A.*, 107, 22722–22727.

Scoffoni, C., Rawls, M., McKown, A., Cochard, H. & Sack, L. (2011). Decline of leaf hydraulic conductance with dehydration: relationship to leaf size and venation architecture. *Plant Physiol.*, 156, 832–843.

Turcotte, D.L., Pelletier, J.D. & Newman, W.I. (1998). Networks with side branching in biology. *J. Theor. Biol.*, 193, 577–592.

Tyree, M.T. & Ewers, F.W. (1991). The hydraulic architecture of trees and other woody plants. *New Phytol.*, 119, 345–360.

Tyree, M.T. & Zimmerman, M. (2002). *Xylem Structure and the Ascent of Sap*. Springer, Berlin.

Warton, D.I., Wright, I.J., Falster, D.S. & Westoby, M. (2006). Bivariate line-fitting methods for allometry. *Biol. Rev.*, 81, 259–291.

Weitz, J.S., Ogle, K. & Horn, H.S. (2006). Ontogenetically stable hydraulic design in woody plants. *Funct. Ecol.*, 20, 191–199.

West, G.B., Brown, J.H. & Enquist, B.J. (1997). A general model for the origin of allometric scaling laws in biology. *Science*, 276, 122–126.

West, G.B., Brown, J.H. & Enquist, B.J. (1999). A general model for the structure and allometry of plant vascular systems. *Nature*, 400, 664–667.

Zamir, M. (2001). Fractal dimensions and multifractility in vascular branching. *J. Theor. Biol.*, 212, 183–190.

Zwieniecki, M.A., Melcher, P.J., Boyce, C.K., Sack, L. & Holbrook, M. (2002). Hydraulic architecture of leaf venation in *Laurus nobilis* L. *Plant Cell Environ.*, 25, 1445–1450.

SUPPORTING INFORMATION

Additional supporting information may be found in the online version of this article:

Appendix S1 Derivation of the expectations for the lattice model equations presented in Table S5, Figs S1–S7 showing histogram of mean edge lengths and total network length (S1) and the performance of each model type (S2–S7).

File S1 Frequency distributions for edge lengths and edge diameters for all 353 leaves (combined into a single pdf).

Table S1 Species List including image ID number, Family, Genus and Species for each leaf image.

Table S2 Individual leaf data, including: image ID number, image scale, leaf area (mm^2), nodes, edges, edges/nodes, mean edge length, total network length, network density (total network length/total leaf area), mean distance to the nearest edge, mean distance to the nearest edge/mean edge length.

Table S3 Edge length and diameter frequency distributions including image ID number, exponential log likelihood, exponential AIC score, maximum likelihood estimate for the exponential rate parameter, power-law log likelihood, power-law AIC score, maximum likelihood estimate for the power-law scaling exponent, maximum likelihood estimate for the power-law scaling constant.

Table S4 Results of the honeycomb, square and equilateral triangular lattice model tests, including predicted edges per unit area, network density, mean distance to the nearest edge, total number of nodes, total number of edges and total network length.

Editor, Marcel Holyoak
Manuscript received 8 June 2011
First decision made 14 July 2011
Second decision made 8 October 2011
Manuscript accepted 11 October 2011